Dual sampling-rate observer-based state feedback control of motor drive systems

--- Estimation from coarse position signal with dead time ----

Takafumi Koseki, Takeomi Suzuki and Lilit Kovudhikurlungsri

Department of Electrical Engineering, School of Engineering, The University of Tokyo

takafumikoseki@ieee.org

Abstract — **This paper describes an effective way to estimate state variables, such as motor speed and disturbance from a low resolution encoder at low speed by using the dual-sampling-rate observer. The dual-sampling-rate observer estimates the state variables at every DSP control period and correct the estimation error at the instant that the measurement signal is detected. A novel pole assignment method, which considers the relation of the estimation and error correction periods, is proposed to maintain the stability for long error correcting period. Moreover, the dual-sampling-rate observer can be applied for higher order systems since it is generalized in state space. The effectiveness of the observer is verified through various simulations and experiments. Furthermore, it briefly describes recent theoretical extension for treating dead-time in the state estimation.**

Keywords — **Dead time, digital observer, estimation, stability, variable sampling rates.**

I. Introduction

Low-resolution encoders are widely used for traction systems such as rolling stocks, electric vehicles, etc. For example, pulse generators used as speed sensors in Japanese commuter trains have only 60 pulses per revolution (ppr). The accuracy remarkably degrades at low speed, where the encoder pulses cannot be detected at every control period. The conventional method to obtain the speed is called the numerical difference method. This method is implemented by measuring the change in angle by counting the pulses produced in a counting period and dividing by the counting period. The resolution will be very coarse in case of a small pulse counting period. Hence, this method is not applicable to a low-resolution encoder of which the pulses are not frequently produced. An alternative way to raise the resolution is to count the time interval between two consecutive pulses [1]. The resolution at low speed is improved, since the interval between two consecutive pulses is relatively long. Conversely, this method has a limitation at high speed. Even though the resolution at low speed is raised, the time delay is unavoidable, since the calculated speed is the average value of the previous interval. Combination of these methods is proposed by Ohmae *et al.* [2]. This method maintains the resolution by combining the advantages of each method. However, the problem of time delay is still unavoidable.

To avoid this problem, it is necessary to estimate the speed between two consecutive pulses. A powerful method to grasp the speed between the encoder pulses is the "instantaneous speed observer" [3].[6]. It is a specific discrete-time observer estimating or predicting the speed based on the plant model, which is the mechanical dynamics of a motor, at every control period and correcting the error of estimation when the next pulse is detected. It has been recently applied in the field of traction control of an electric vehicle [5] and rolling stock control [7]-[9]. One of the difficulties in traction control is that it deals with a wide range of speeds. The observer gains were tuned by simply considering only the relation of pole locations on s- and z-planes [4], [8]-[10]. As a result, the system can operate stably in a wide range of speed except at extremely low speed, where pulses cannot be detected frequently. Improvement of the speed estimation can be done by careful consideration of the pulse detection timing [6]. However, the stability issue of the observer is not clarified.

The instantaneous speed observer can be categorized as a multirate sampling observer, since the error-correction period is longer than the estimation period. The multirate sampling theory [11]-[13] has been applied in industrial application such as position control of hard disk drive

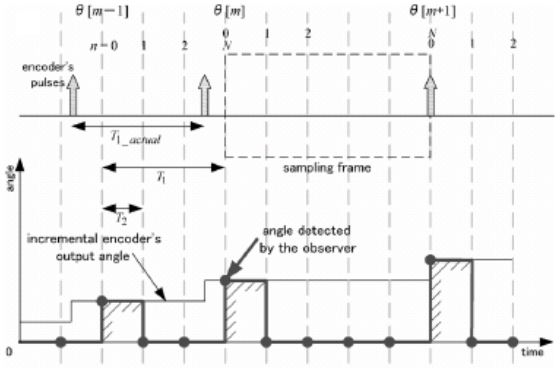

Fig. 1. Timing diagram of the dual-sampling-rate observer when the period between two consecutive pulse is larger.

[14] where the sampling period of plant output is restricted to be relatively longer than the control period of plant input. This method, however, deals with a constant ratio of sampling times. It is different from the instantaneous speed observer where the error correction period varies with the motor speed.

In order to analyze the instantaneous speed of the observer [15], the concept of multirate sampling theory [11]-[14] is applied by taking into account the variation of the ratio of the sampling periods. The stability in ultra-low-speed range can be maintained by careful consideration of the relation of estimation- and error correction period. Gain calculation, however, is quite complicated since it needs gain recalculation to stabilize the observer in ultra low speed range.

The observers mentioned in [3]-[9], [15] are the predicting observers, which used the detected output of the previous sampling instant to correct the estimation error. The observer that uses the current detected output to correct the estimation error is defined as the current observer [16]. By rearranging the instantaneous speed of the observer based on the current observer; the authors found out a more simple gain calculation that still maintains the performance of the observer[17].

In this paper, the instantaneous speed observer in state space is generalized. Since it has two sampling periods: error correction period T_1 and the estimation period T_2 it can be defined as "dual-sampling-rate observer." Its principle is introduced in Section II. Derivation and pole assignment of the predicting Dual-sampling-rate observer is reviewed in Section III. The effectiveness of the observers is verified through various simulations and experiments in Section IV. Furthermore, the observer is extended to estimate stably the state variables of an asymptotically stable plant which has considerable dead time in an output signal path in Section V based on the predictive dual-rate sampling observer.

Table 1 Nomenclature

Symbol	Description
$\mathbf{A}$	Coefficient matrix a state vector
$\mathbf{B}$	Coefficient matrix a input vector
$\mathbf{C}$	Coefficient matrix a output vector
J	Moment of inertia
$\mathbf{L}$	Conventional observer's gain matrix
$\mathbf{L}^*$	Dual-sampling-rate observer's gain matrix
N	Amount of sampling instants in a sampling frame or last sampling instant a sampling frame
T_{1_actual}	Actual interval between two consecutive pulses
T_1	Interval between two consecutive pulses read by the DSP
T_2	Control period
T_L	Load torque
T_m	Motor torque
c	Friction , viscosity of the damper
$\mathbf{e}$	Estimation error vector
g_r	Gear ratio
k	Spring constant
m	Index number of the pulse or sampling frame
n	Sampling instant in a sampling frame
q	Number of poles of the observer
u or $\mathbf{u}$	Input or input vector
x or $\mathbf{x}$	State variable or state vector
$\hat{\mathbf{x}}$	Estimated or corrected state vector
$\tilde{\mathbf{x}}$	Predicted state vector
y or $\mathbf{y}$	Measurement output or measurement output vector
z	Pole on z-plane
θ	Shaft angle or motor angle
ω	Motor angular speed

II. Principle of the Dual-Sampling-Rate Observer

The principle of the dual-sampling-rate observer is to predict the state variables at every sampling time based on the angle when the pulse is detected and correct the error when the next encoder pulse is detected. Fig. 1 shows a timing diagram of the output of an incremental encoder and the angle detected by the dual-sampling-rate observer. T_{1_actual} , T_1 , and T_2 denote the actual interval between two consecutive pulses, the interval between two consecutive pulses read by the DSP and the control period, respectively. Bold arrows stand for pulses generated by the encoder. It is seen from the figure that the incremental encoder output angle is instantaneously updated when a pulse is detected. This signal is, however, read at the next sampling instant. Therefore, there occurs unavoidable delay. This signal is held for one control period and then reset to zero based on the principle of the observer.

Next, let us consider the case when the motor starts acceleration. The encoder generates the pulses more frequently when the interval between two consecutive pulses that the DSP reads becomes smaller than the control period the pulses can be detected at every control period. In this case, T_1 is equal to T_2 . As a result, the dual-sampling-rate observer predicts and corrects the error at every sampling instant. Therefore, we can conclude that the dual-sampling-rate observer becomes an

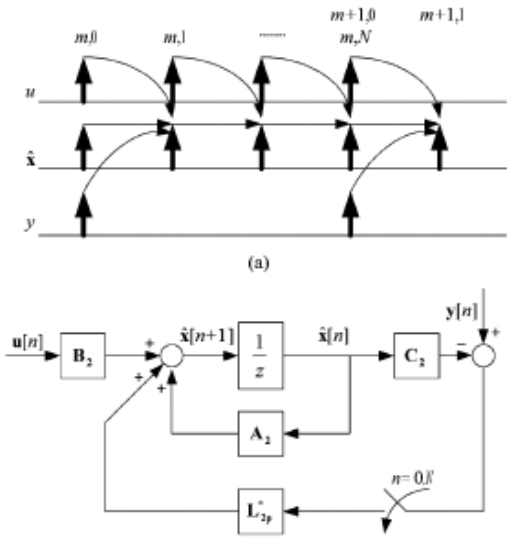

Fig. 2. Timing diagram of the dual-sampling-rate observer when the period between two consecutive pulse is larger.

ordinary discrete-time observer when the interval between two consecutive pulses is smaller than the control period.

The dual-sampling-rate observer can be separated into two types according to the structure: the predicting type that uses the encoder pulse, i.e., the measurement signal, to correct the next state, and the current type, that uses the current measurement signal to correct the current state. The signal and block diagrams of the predicting type are shown in Fig. 2. The variables $\hat{\boldsymbol{x}}$, $\boldsymbol{u}$, and $\boldsymbol{y}$ denote the estimated or corrected state, the input and the measurement vectors, respectively. A_2, B_2, C_2, $L_{2\mathrm{p}}^*$ denote the matrices in discrete-time domain sampled by T_2. The subscript 2 indicates that the constant control period T_2 is used as the sampling time. The subscript p denotes predicting type.

III. Predicting Dual-Sampling-Rate Observer

A. Derivation

According to Fig. 1, the sampling instant [m, n] is defined by

$$t = m\,T_1(\theta[m]) + n\,T_2 = [m, n] \tag{1}$$

where $\theta[m]$, m, and n denote the shaft angle, the index number of the pulses, and the sampling instant the counting of which starts when a pulse is detected and reset when the next pulse is detected, respectively. The value of n is between 0 and N, where N denotes last sampling instant. The relationship between the sampling indices m and n can be concluded as

$$[m, N] = [m+1, 0]\,. \tag{2}$$

$$\hat{\boldsymbol{x}}[n+1] = \begin{cases} A_2\hat{\boldsymbol{x}}[n] + B_2\boldsymbol{u}[n] + L_{2\mathrm{p}}^*(\boldsymbol{y}[n] - C_2\hat{\boldsymbol{x}}[n]), & n=0 \\ A_2\hat{\boldsymbol{x}}[n] + B_2\boldsymbol{u}[n], & n=1,2,\ldots,N-1 \end{cases} \tag{3}$$

Other symbols are explained in Table 1. It is also convenient to define an interval between two consecutive pulses as a "sampling frame". Thus, (2) implies that the *N*-th sampling instant of the current sampling frame is the zeroth sampling instant of the next sampling frame and m is the index number of the sampling frame.

According to the signal diagram in Fig. 2, when an encoder pulse is detected, the error of estimation is corrected.

On the other hand, when pulses are not detected, the observer principally works as a simulator, predicting the state variables based on the plant model as shown in (3) at the bottom of the page, where A_2, B_2, C_2, and $L_{2\mathrm{p}}^*$ denote matrices in discrete time domain sampled by T2. The subscript 2 indicates that the constant control period T2 is used as the sampling time. It is very important to note that the disturbance is included in the state vector for accurate estimation. The block diagram of the predicting dual-sampling-rate observer is shown in Fig. 2(b). Rearranging (3) based on the sampling instant $n=0$, the state variable can be expressed as

$$\begin{aligned} \hat{\boldsymbol{x}}[n] = {} & A_2^n\boldsymbol{x}[0] + A_2^{n-1}B_2\boldsymbol{u}[0] + A_2^{n-2}B_2\boldsymbol{u}[1] \\ & + \ldots + A_2^0 B_2\boldsymbol{u}[n-1] \end{aligned} \tag{4}$$

B. Pole Assignment

Pole assignment is achieved by a consideration of the error dynamics of the observer. To do this, it is necessary to rearrange the state vector of the plant in terms of the last-sampling-instant state vector of the previous sampling frame as

$$\boldsymbol{e}[m+1] = (A_2^N - A_2^{N-1}L_{2\mathrm{p}}^*C_2)\boldsymbol{e}[m] \tag{5}$$

At the instant when the next pulse is detected, *i.e.*, $n=N$, subtracting (5) from (4) and using the relation (2), the error of estimation e of a sampling frame can be expressed as

$$\boldsymbol{e}[m+1] = (A_2^N - A_2^{N-1}L_{2\mathrm{p}}^*C_2)\boldsymbol{e}[m] \tag{6}$$

Consequently, the observer gains are obtained by placing the poles in the unit circle and solving the equation

$$\prod_{i=1}^{q}(x - z_i) = |z\boldsymbol{I} - A_2^{N-1}(A_2 - L_{2\mathrm{p}}^*C_2)| \tag{7}$$

where size z_i and q denotes the *i*-th pole on z-plane and the number of poles, respectively.

Equation (7) is very useful in pole assignment as it guarantees that the actual pole of the observer is placed as shown in Fig. 3(c) and (d). This maintains the stability of the system as shown in Fig. 3(a) and (b). An example when (7) is not used in pole placement is shown in Fig. 4. The observer gain is calculated by fixing the pole on s-plane and transform to z-plane by using T_1 as the sampling time. It is seen that an actual pole of the observer moves outward the unit circle, even though the poles moves inside the unit circle in the design. As a result, the control system cannot operate stably.

C. Comparison to the Conventional Method

T_1 is defined as the period between two consecutive pulses detected by the observer, so it is variable. When dealing with a variable-sampling-time system, the controller and the observer are conventionally designed by using T_1 as the sampling times.

The conventional predicting observer equation is described by

$$\hat{\boldsymbol{x}}[m+1] = A_1\hat{\boldsymbol{x}}[m] + B_1\boldsymbol{u}[m] + L_{1\mathrm{p}}(\boldsymbol{y}[m] - C_1\hat{\boldsymbol{x}}[m]) \tag{8}$$

Note that subscript 1 indicates that T_1 is used as a sampling time. The observer gain is conventionally obtained as

$$\prod_{i=1}^{q}(x - x_i) = |z\boldsymbol{I} - (A_1 - L_{1\mathrm{p}}C_1)| \tag{9}$$

Using the fact that $A_2^N = A_1$ and $C_2 = C_1$, and comparing (9) and (7), the relation of the observer gain matrices of the dual sampling-rate observer and the

discrete-time observer, where T_1 is the sampling time given by

$$L_{2p}^{*}=(A_2^{N-1})^{-1}L_{1p} \tag{10}$$

where A_2^{N-1} is always nonsingular. By this fact, it is possible to calculate the observer gain of the dual-sampling-rate observer by the conventional method and then converting by (10) to stabilize the predicting dual-sampling-rate observer.

D. Gain Calculating Procedure

The gains of the observers can be simply calculated by consideration of the relationship of the observer gain matrices in (10). The gain calculating procedure is concluded as follows in two steps.

Step1: Placing the poles and calculating the observer gain matrix L_{1p} by the conventional method.

Step2: Using the relationship in (10) to calculate the accurate observer gain matrix of the dual-sampling rate observer L_{2p}^{*}.

The observer gain matrix of the predicting type L_{2p}^{*} varies according to N, which is the number of the inter-sampling, or the ratio of T_1 to T_2. In practice, we can easily apply this gain tuning by off-line calculation and storing the calculated gain matrix in a look-up table.

In the current-type dual-sampling rate observer described in [17], the gain calculation is substantially simplified: Step 2 can be omitted for the current type, in practice, since the gains are identical. Hence, it is not necessary to prepare the gain table in advance. This is the major advantage of the current type.

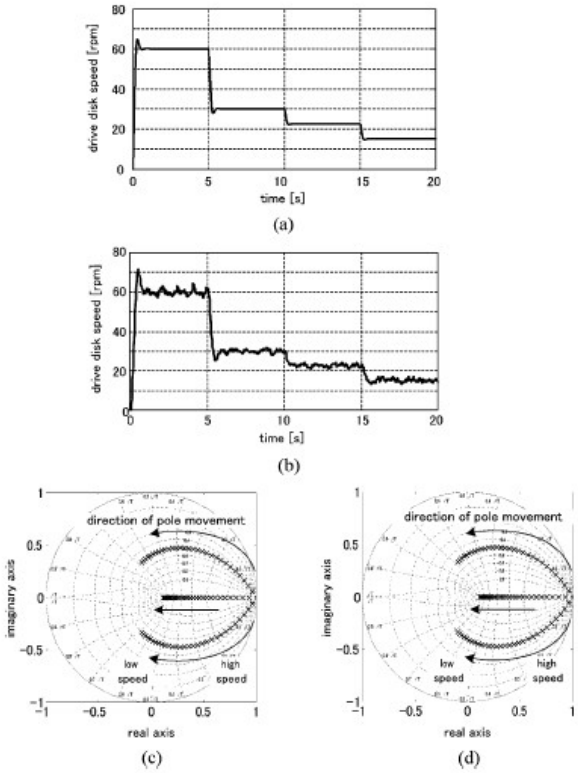

Fig. 3 (a) Simulation and (b) experimental results of the proposed pole assignment. (c) Movement of the poles in design. (d) Actual movement of the poles.

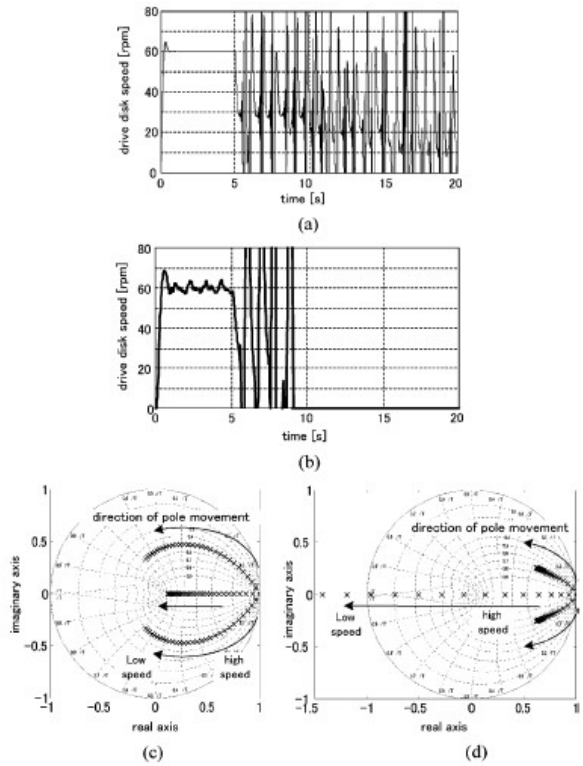

Fig. 4 (a) Simulation and (b) experimental results of the conventional pole assignment. (c) Movement of the poles in design. (d) Actual movement of the poles.

IV. Numerical and Experimental Verification

The dual-sampling-rate observer and the proposed pole assignment have been verified by the experimental apparatus shown in Fig. 5. It is composed of an inertia-adjustable drive disk driven by a brush-less dc motor and an inertia-adjustable load disk. Belts connect both disks to each other via a speed reduction gear set. 16,000-ppr rotary encoders are installed to measure the speed of each disk, but the resolution for the control is reduced to 80 ppr to verify the performance of the observer. The control

Table 2 List of experimental parameters.

Symbol	Quantity	Value
c_D	Drive friction	0.004 Nm/rad/s
c_L	Load friction	0.05 Nm/rad/s
g_r	Gear ratio	4
J_D	Drive inertia and gear set inertia	0.00252 kgm^2
J_L	Load inertia	0.0271 kgm^2
K_{DL}	Flexible belt's equivalent torsional spring constant	8.45 Nm/rad

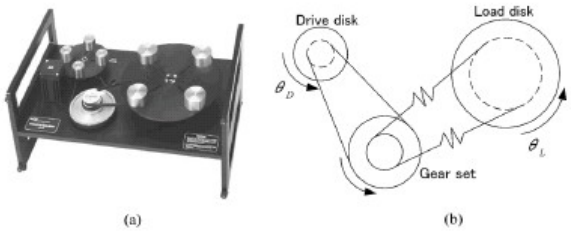

Fig. 5 (a) Experimental apparatus. (b) Free body diagram.

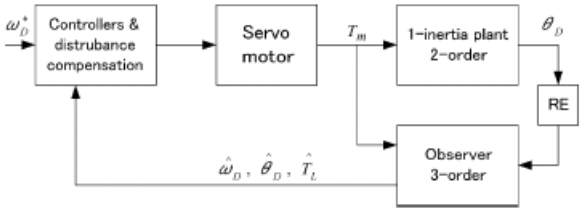

Fig. 6. Block diagram for verification of the pole assignment method.

period is set to 1.768 ms. Experimental constants are summarized in Table 2.

The objectives of the verification is to verify the effectiveness of the proposed pole assignment.

For simplicity, the proposed pole assignment method is verified based on a one-inertia system. The plant transfer function is described as

$$\frac{\omega_D(s)}{T_m(s)}=\frac{1}{J_D s+c_D} \tag{11}$$

where T_m denotes the motor torque. The controller is designed such that the equivalent time constant of the system is 200 ms. Consequently, the third-order observer is enough to estimate the whole state variables including disturbance. Its state equation is expressed in (3) for the predicting type, where the state, input, and output vectors are described as .

$$\hat{\boldsymbol{x}}=[\hat{\theta}_D \;\; \hat{\omega}_D \;\; \hat{T}_L]^T \quad , \quad \boldsymbol{u}=T_m \quad , \quad \hat{\boldsymbol{y}}=\hat{\theta}_D \tag{12}$$

where $\hat{\theta}_D$, $\hat{\omega}_D$, and . T_L denotes the drive disk's angle, speed and the load torque. Coefficient matrices A_2 , B_2 , and C_2 in (3) are derived from their continuous-time domain matrices with zeroth-order disturbance consideration A_{cd3} , B_{cd3} , and C_{cd3} , respectively. The subscript 3 means third order. The components of these matrices are described as

$$A_{cd3}=\begin{bmatrix} 0 & 1 & 0 \\ 1 & 0 & \frac{1}{J_D} \\ 0 & 0 & 0 \end{bmatrix} \quad , \quad B_{cd3}=\begin{bmatrix} 0 \\ \frac{1}{J_D} \\ 0 \end{bmatrix} \quad ,$$

$$C_{cd3}=[1 \;\; 0 \;\; 0] \tag{13}$$

Note that the friction factor c_D in (11) is considered as a disturbance so it is not expressed in the state transition matrix in (13). Fig. 6 shows the block diagram of the controlled system. It is important to note that the interval between two consecutive pulses produced from the rotary encoder changes according to speed. In many systems, where an ordinary discrete-time observer is implemented, the observer is conventionally designed at nominal operating speed by placing the poles on s-plane so that the desirable settling time is obtained and then mapping the poles on the s-plane to the z-plane by using the interval between the pulses T_1 as the sampling time [4]. In the case of a wide-speed-range system, the observer poles may be changed according to the speed in order to maintain the relationship between the time constant of the system and the observer. Note that the poles of the instantaneous speed observer, which are similar to the third order predicting dual-sampling-rate observer, was previously placed by this method. The results and pole locations in the case when the poles of the observer are designed by the conventional method are shown in Fig. 4.

The time constant of the observer is twice as fast as that of the system at any speed. However, the system cannot be stably driven when the speed drops below 60 r/min. This is because the poles are fixed on the s-plane and mapped to the z-plane without consideration of the relation of T_1 and T_2 . Fig. 4(c) and (d) shows the movements of the observer poles in design and actual pole movements, respective. It is obviously seen in Fig. 4(d) that an actual pole of the observer moves onto the negative real axis when the speed drops below 53 r/min and proceeds to the outward direction of the unit circle. This confirms the fact that placing the poles without considering the relationship between the two sampling times causes instability. One way to solve this instability problem is to fix the poles on z-plane and reduce the controller gains to maintain the ratio of the time constant between the observer and the controlled system. But this will result in slow response of the system [9].

Fig. 3 shows the results and pole locations by using the proposed pole assignment method. It is seen that by using the relation in (10) the gains are adjusted so that the poles move inside the unit circle on both z-planes, as shown in Fig. 3(c) and (d). Hence, the system can operate stably, as shown in Fig. 3(a) and (b). Note that the speed of 15 rpm corresponds to the pulse interval T_1 of 50 ms in case of the encoder's resolution of 80 ppr and the control period T_2 is set to 1.768 ms. In other words, T_1 is 28 times greater than T_2 . This emphasizes the fact that the proposed pole assignment method maintains the stability and allows us to design a fast controller even at low speeds so that the desirable response can be achieved.

V. Extension to the State Estimation of a Stable System with Considerable Dead Time in Output Signals

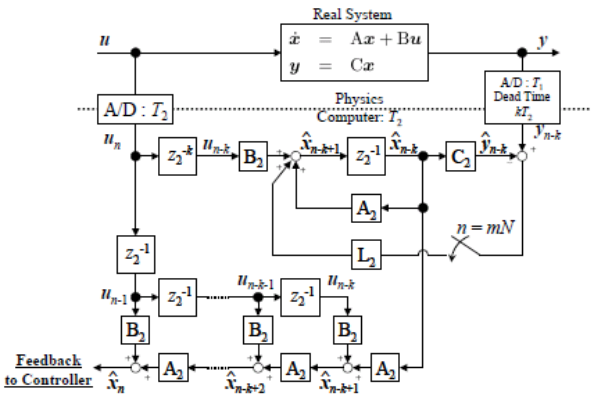

Fig. 7. Block diagram for estimating state variables of a plant with dead time in output signal path.

It is known that dead time in a plant often causes instability in feedback controls. By extending the idea of the dual-sampling rate observer as shown in Fig. 7, guaranteeing stable state estimation is possible for an asymptotic stable plant with dead time in output signal path, by continuing internal delayed state estimation represented by $\hat{x}_n$, and calculating present estimated present state variable $\check{x}_n$ by extrapolating $\hat{x}_n$ based on internal plant model in the observer for actual state feedback. This idea will be useful in recent technologies of visual servos, and remote operations through a communication network.

VI. Conclusions

This paper describes an effective way to achieve precise inter-sampling estimation from an event-based sampling system such as traction control, in which a low-resolution encoder are commonly used as the speed sensors, by introducing dual-sampling-rate observer. Its principle is to estimate or predict the state variables between the encoder pulses based on model-based knowledge of physical plant dynamics and correct the estimation error when the next encoder pulse is generated. It is classified into two types based on its structure: the predicting type and the current type. It can be extended for estimating a high-order plant easily, since it has been generalized in state space representation. This extension has allowed us to estimate the whole state variables. This has made the design of state feedback possible, and the control performance was improved from that of the conventional methods. The observer has two sampling times: the constant period of estimation T_2 equal to the control period and the variable period of error correction T_1 equal to the pulse interval detected by the observer. This has lead to the proposal of a novel pole assignment method that stabilizes the operation of the observer in all speed range by considering the relationship between T_1 and T_2 .

We have also found the relationship between the observer gains of the dual-sampling-rate observer and the variable-sampling single- rate observer, sampled by T_1 . This relationship has simplified the gain calculating procedure, especially in the case of the current type where the observer gain is identical to the variable-sampling-single-rate observer, sampled by T_1 .

The idea can be applied to not only a motor but also any high-order plants.

References

[1] R. D. Lorenz, "Microprocessor control of motor drive and power converters," Microprocessor Motion Control of AC and DC Drive, IEEE Tutorial Course Note Book from 1991, 1992 and 1993, IEEE, IAS Annual Meetings, IEEE Publishing Services #THO587-6.

[2] T. Ohmae, T. Matsuda, K. Kamiyama, and M. Tachikawa, "A microprocessor-controlled high-accuracy wide-range speed regulator for motor drives," IEEE Trans. Ind. Electron., vol. IE-29, no. 3, pp. 207-221, Aug. 1982.

[3] Y. Hori, "Robust motion control based on a two-degrees-of-freedom servosystem," Adv. Robot., vol. 7, no. 6, pp. 525-546, 1993.

[4] S. Sakai and Y. Hori, "Ultra-low speed control of servomotor using low resolution rotary encoder," in Proc. 1995 IEEE IECON 21st Int. Conf. Ind. Electron., Control, Instrum., Orlando, FL, Nov. 1995, vol. 1, pp. 615-620.

[5] G. Guidi, H. Kubota, and Y. Hori, "Induction motor control for electric vehicle application using low resolution position sensor and sensorless vector control technique," in Proc. Power Convers. Conf.,Nagaoka, Japan, 1997, pp. 937-942.

[6] S. Lee, T. Lasky, and S. Velinsky, "Improved velocity estimation for lowspeed and transient regimes using low-resolution encoders," IEEE/ASME Trans. Mechatronics, vol. 9, no. 3, pp. 553-560, Sep. 2004.

[7] M. Cao, K. Takeuchi, T. Furuya, and A. Kawamura, "Adhesion control in low-speed region and experiment verification with considering low.resolution pulse generator," in Proc. Power Convers. Conf., Osaka, Japan, 2002, pp. 873-878.

[8] L.Kovudhikulrungsri and T.Koseki, "Speed estimation of induction motor in low speed for pure electric brake," in Proc. Transp. Electr. Railways Linear Drive Conf., Sapporo, Japan, Jul. 2000, pp. 19-24.

[9] "Control of an induction motor for pure electric brakes," in Proc. 2001 Jpn. Ind. Appl. Soc. Conf., Matsue, Japan, Aug. 2001, vol. 3, pp. 1297-1303.

[10] "Precise speed and torque control for AC traction pure electricbraking system in lowspeed range," Trans. Inst. Electr.Eng. Jpn., vol. 122- D, no. 11, pp. 1027-1033, 2002.

[11] M. Araki and T. Hagiwara, "Multivariable multirate sampled-data system: state-space description, transfer characteristics and Nyquist criterion," IEEE Trans. Autom. Control, vol. AC-31, no. 2, pp. 145-154, Feb. 1986.

[12] M. Araki and K. Yamamoto, "Pole assignment by multirate sampleddata output feedback," Int. J. Control, vol. 44, no. 6, pp. 1661-1673, 1986.

[13] H. M. Al-Rahmani and G. F. Franklin, "Multirate control: A new approach," Automatica, vol. 28, no. 1, pp. 35-44, 1992.

[14] H. Fujimoto and Y. Hori, "High performance servo systems based on multirate sampling control," Int. Fed. Autom. Control J. Control Eng. Practice, vol. 10, no. 7, pp. 773-781, 2002.

[15] L. Kovudhikulrungsri and T. Koseki, "Improvement of performance and stability of a drive system with a low-resolution position sensor by multirate sampling observer," Trans. Inst. Elect. Eng. Jpn., vol. 124-D, no. 9, pp. 886-892, 2004.

[16] A. Tewari, Modern ControlDesign withMATLAB and SIMULINK. New York: Wiley, 2002.

[17] L. Kovudhikulrungsri and T. Koseki, "Precise Speed Estimation From a Low-Resolution Encoder by Dual-Sampling-Rate Observer," IEEE/ASME Trans. on Mechatronics, Vol. 11, No. 6., pp. 661-670, 2006